The Plant Cell, Vol. 14, 1293–1309, June 2002, www.plantcell.org © 2002 American Society of Plant Biologists

Membrane Protein Transport between the Endoplasmic Reticulum and the Golgi in Tobacco Leaves Is Energy Dependent but Cytoskeleton Independent: Evidence from Selective Photobleaching

Federica Brandizzi,[a,1] Erik L. Snapp,[b] Alison G. Roberts,[c] Jennifer Lippincott-Schwartz,[b] and Chris Hawes[a]

[a] Research School of Biological and Molecular Sciences, Oxford Brookes University, Gipsy Lane, Oxford OX3 0BP, United Kingdom

[b] Cell Biology and Metabolism Branch, National Institute of Child Health and Human Development, National Institutes of Health, Bethesda, Maryland 20892

[c] Scottish Crop Research Institute, Dundee DD2 5DA, United Kingdom

The mechanisms that control protein transport between the endoplasmic reticulum (ER) and the Golgi apparatus are poorly characterized in plants. Here, we examine in tobacco leaves the structural relationship between Golgi and ER membranes using electron microscopy and demonstrate that Golgi membranes contain elements that are in close association and/or in direct contact with the ER. We further visualized protein trafficking between the ER and the Golgi using Golgi marker proteins tagged with green fluorescent protein. Using photobleaching techniques, we showed that Golgi membrane markers constitutively cycle to and from the Golgi in an energy-dependent and *N*-ethylmaleimide–sensitive manner. We found that membrane protein transport toward the Golgi occurs independently of the cytoskeleton and does not require the Golgi to be motile along the surface of the ER. Brefeldin A treatment blocked forward trafficking of Golgi proteins before their redistribution into the ER. Our results indicate that in plant cells, the Golgi apparatus is a dynamic membrane system whose components continuously traffic via membrane trafficking pathways regulated by brefeldin A– and *N*-ethylmaleimide–sensitive machinery.

INTRODUCTION

After translocation into the endoplasmic reticulum (ER), most proteins exported for secretion must pass through the Golgi apparatus before reaching their final destination within the secretory pathway. Despite great strides in understanding the molecular and organizational properties of the secretory pathway in animal cells (Rothman and Wieland, 1996; Schekman and Orci, 1996; Barlowe, 2000; Lippincott-Schwartz et al., 2000), comparable information on secretory transport pathways in plant cells is only just emerging (Hawes et al., 1999). Genome analysis (Andreeva et al., 1997) and biochemical/immunological studies (Pimpl et al., 2000; Phillipson et al., 2001; Ritzenthaler et al., 2002) have shown that components of the COPI and COPII coat systems (Schekman and Orci, 1996; Barlowe, 2000), which are proposed to function in vesicle transport in animal cells (Rothman and Wieland, 1996), operate in protein trafficking steps in plant cells. For example, GTPase-deficient mutants of Sar1, Rab1, and ARF1 have been shown in plant cells to act as *trans*-dominant negative inhibitors of protein transport (Andreeva et al., 2000; Batoko et al., 2000; Takeuchi et al., 2000; Phillipson et al., 2001). Moreover, immunogold labeling of cryosections has shown that COPI and ARF1 are localized to small vesicles surrounding or budding from cisternae at the *cis* face of the Golgi apparatus in plant cells and that the binding of these proteins is sensitive to brefeldin A (BFA) (Pimpl et al., 2000; Ritzenthaler et al., 2002).

Despite the similarities in the secretory trafficking machinery of plants and animals, the behavior of secretory organelles such as the ER and the Golgi is dramatically different in the cells of these two kingdoms. In vivo imaging of leaf tissue has revealed an intimate relationship between the ER and the Golgi in these cells (Boevink et al., 1998; Saint-Jore et al., 2002). Golgi stacks were found to move rapidly and extensively along the ER, with an actomyosin system propelling the Golgi stacks along the ER network (Boevink et al., 1998; Nebenführ et al., 1999). A variety of models have been proposed to explain how ER-to-Golgi protein transport occurs under these conditions. One

[1] To whom the correspondence should be addressed. E-mail fbrandizzi@brookes.ac.uk; fax 44-1865-483955.

Article, publication date, and citation information can be found at www.plantcell.org/cgi/doi/10.1105/tpc.001586.

proposal is that the rapid Golgi movement in plant cells allows the Golgi to continually collect vesicles budding from the ER (the vacuum cleaner model; Boevink et al., 1998). In this view, vesicles are thought to bud out from the ER, so Golgi bodies must continually move to collect them.

A second model is that Golgi stack movement allows the Golgi to move between fixed ER exit sites (the stop-and-go model; Nebenführ et al., 1999). In this view, cargo collection would occur only when Golgi stacks stop at ER exit sites, possibly after transient detachment from actin. A third possibility is that Golgi movement represents the movement of both ER and Golgi stacks that behave as one dynamic system, either through direct membrane continuities or through continuous vesicle or tubule formation/fusion reactions. Golgi movement in this model would represent the dynamic movement of the secretory apparatus itself, allowing cargo to be delivered throughout the plant cell. A close opposition between ER export sites and the Golgi apparatus has been indicated in *Pichia pastoris* and mammals (Rossanese et al., 1999; Hammond and Glick, 2000).

These findings, and the accompanying models they have produced, have led to an intense interest in characterizing ER/Golgi trafficking in plant cells. The development and application of green fluorescent protein (GFP) technology has provided an important new approach to the characterization of protein trafficking pathways in living cells (Lippincott-Schwartz et al., 2000). GFP can be fused with a native or foreign cellular protein, or targeting peptide. When expressed in living cells, these proteins allow direct visualization of the behavior of their target organelles (for review, see Hawes et al., 2001; Lippincott-Schwartz et al., 2001). Furthermore, photobleaching techniques allow the movement of GFP-tagged proteins between and within organelle(s) to be studied (Ladha et al., 1996; Lippincott-Schwartz et al., 2001).

In this study, we used electron microscopy and GFP-based techniques to gain insight into the relationship of ER and Golgi bodies and the protein-trafficking pathways that operate between them in plant cells. GFP chimeras targeted to the ER/Golgi system in *Nicotiana* leaf tissue cells were used in time-lapse imaging and photobleaching experiments to study the trafficking pathways between the ER and the Golgi and the role of energy-dependent, BFA-sensitive, and *N*-ethylmaleimide (NEM)–sensitive factors in these pathways.

RESULTS

Localization of AtERD2-GFP and ST-GFP in Golgi and ER Membranes of Plant Cells

To visualize ER and Golgi membranes in plant cells, we transiently transformed tobacco leaf epidermal cells with GFP spliced to the Arabidopsis HDEL receptor homolog (AtERD2-GFP; Saint-Jore et al., 2002) or to the signal anchor of a rat sialyl transferase (ST-GFP; Batoko et al., 2000; Saint-Jore et al., 2002). ST-GFP– and AtERD2-GFP–expressing cells both showed small fluorescent punctate structures when viewed by confocal fluorescence microscopy (Figures 1A and 1B). These structures have been identified previously as individual Golgi stacks based on immunogold and immunofluorescence labeling (Boevink et al., 1998; Saint-Jore et al., 2002). At high magnification, many of the Golgi stacks/bodies showed dim fluorescent projections or tails (Figures 1C and 1D, arrows). In addition to labeling Golgi stacks, the chimeras were present within ER membranes. The ER pool of AtERD2-GFP (Figure 1B) was much greater than that of ST-GFP, and it distributed as an elaborate polygonal network that was associated closely with Golgi stacks. In time-lapse sequences, the Golgi stacks visualized by ST-GFP (Figures 1E to 1H) or AtERD2-GFP (Figures 1I to 1L) alternated between random saltatory and directional movements in the cortex of the cells, as described previously (Boevink et al., 1998; Batoko et al., 2000; see also movies at http://www.brookes.ac.uk/schools/bms/research/molcell/hawes/gfpmoviepage.html).

To confirm that ST- and AtERD2-protein fusions target the same population of Golgi stacks, an AtERD2–yellow fluorescent protein fusion (AtERD2-YFP; Figure 1N) was coexpressed in the same cells as the ST-GFP fusion (Figure 1M), and all of the Golgi stacks were labeled (Figure 1O).

Relationship between Golgi Stacks and the ER

Previously, Boevink et al. (1998) described the movement of Golgi stacks over the cortical ER network in tobacco leaves. We performed high-resolution time-lapse imaging of AtERD2-GFP expressed in a leaf trichome of *Nicotiana clevelandii* (Figure 2) to study in more detail the intimate relationship between Golgi stacks and the ER. Golgi stacks frequently were found associated with the three-way junctions of ER tubules, where they often remained stable for tens of seconds. Occasionally, individual stacks appeared to break free from the cortical ER network and traverse the cytoplasm before rejoining the network (Figure 2A, arrows). These Golgi stacks often appeared to have a short tail of tubular membrane trailing behind them, as if a small portion of the ER was still attached (Figure 2A, arrows). Likewise, Golgi bodies could break free from the ER and be propelled unidirectionally (Figure 2B, arrow) only to be followed by the growth of an ER tubule following exactly the same trajectory (Figure 2B, large arrow). These findings suggest the Golgi stack movement and ER remodeling are related processes.

The continuous close association of the Golgi with the ER observed by fluorescence microscopy led us to investigate at the ultrastructural level the spatial relationship of these two organelles. We used a zinc iodide/osmium tetroxide fixation protocol (Hawes et al., 1981) to selectively stain the ER and the Golgi (Figure 3). A gradient of staining of Golgi

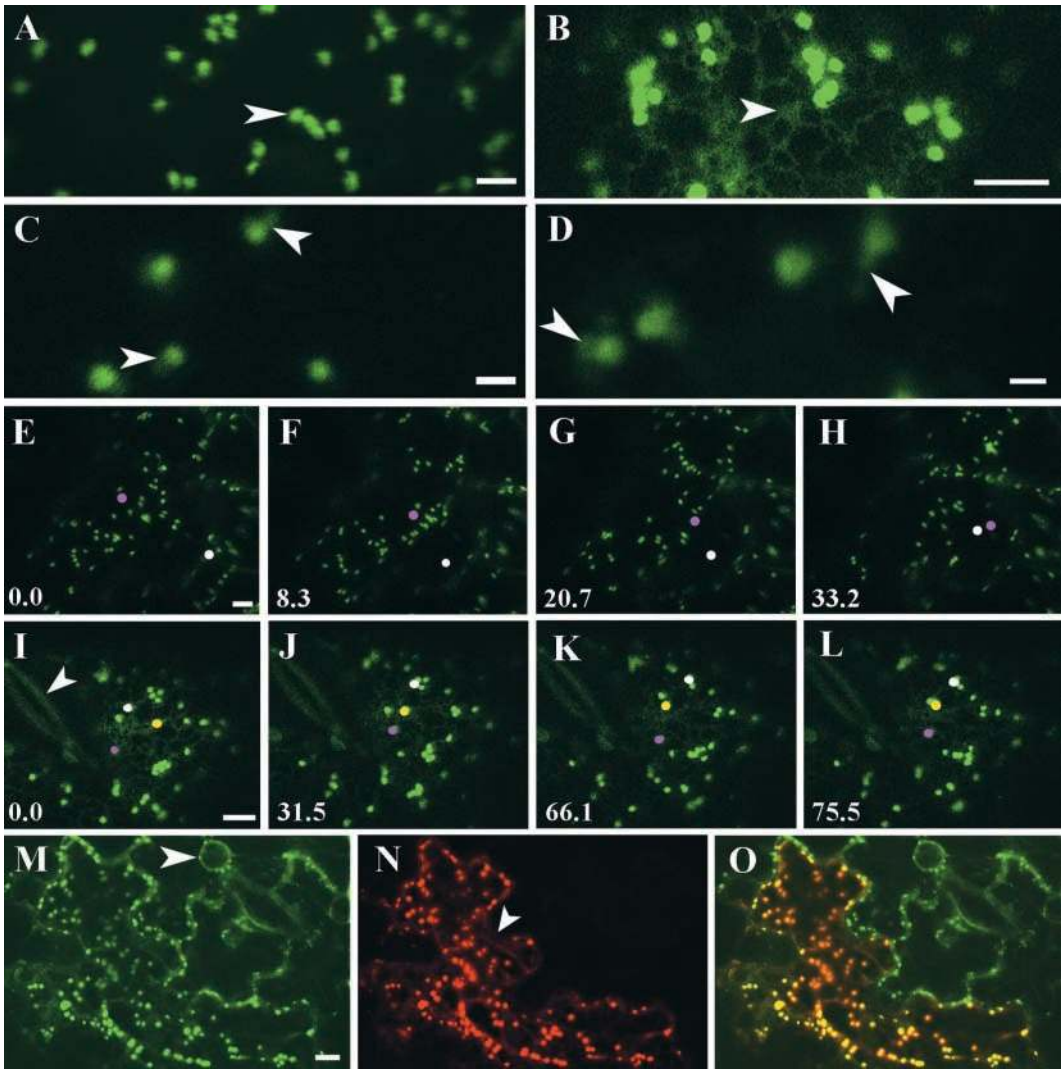

Figure 1. ST- and AtERD2-Fluorescent Markers Label the Same Highly Mobile Population of Golgi Stacks.

(A) In ST-GFP–transformed epidermal tobacco cells, fluorescent Golgi stacks are visible (arrowhead). Bar = 5 μm.

(B) Fluorescent Golgi stacks also are visible in AtERD2-GFP–transformed epidermal cells. The ER network is visible in these cells (arrowhead). Bar = 5 μm.

(C) and **(D)** At higher magnification, wide-open pinhole, and no averaging microscope settings, structures elongating from Golgi stacks are visible (arrowheads) in tobacco cells expressing ST-GFP (**[C]**; bar = 2 μm) and AtERD2-GFP (**[D]**; bar = 1 μm).

(E) to **(H)** Golgi stacks appear highly mobile. In an epidermal cell expressing ST-GFP, the color of two Golgi bodies has been digitally superimposed with pink and white to allow their movement to be followed within a cell in a time lapse. Time is expressed in seconds at the bottom left of each frame. Bar = 5 μm.

(I) to **(L)** Time lapse of a tobacco epidermal cell transformed with AtERD2-GFP near a pair of untransformed guard cells (**[I]**, arrowhead). The color of three Golgi bodies has been digitally superimposed with white, yellow, and pink to allow the movement of the stacks to be followed within the cell. Time is expressed in seconds at the bottom left of each frame. Bar = 5 μm.

(M) to **(O)** Images of a tobacco epidermal cell transformed with ST-GFP and AtERD2-YFP taken with different excitation/emission microscope configurations specific for imaging the two fluorochromes independently. Bar = 5 μm.

(M) Image taken with GFP settings showing the Golgi in cells transformed with ST-GFP. In transiently expressing ST-GFP cells, nuclear envelopes rarely are visible (arrowhead).

(N) Same frame as in **(M)** imaged with YFP settings showing an AtERD2-YFP. The ER network underlying the Golgi stacks is visible (arrowhead).

(O) Merged **(M)** and **(N)** images. Colocalization of GFP and YFP is visible as orange-yellow.

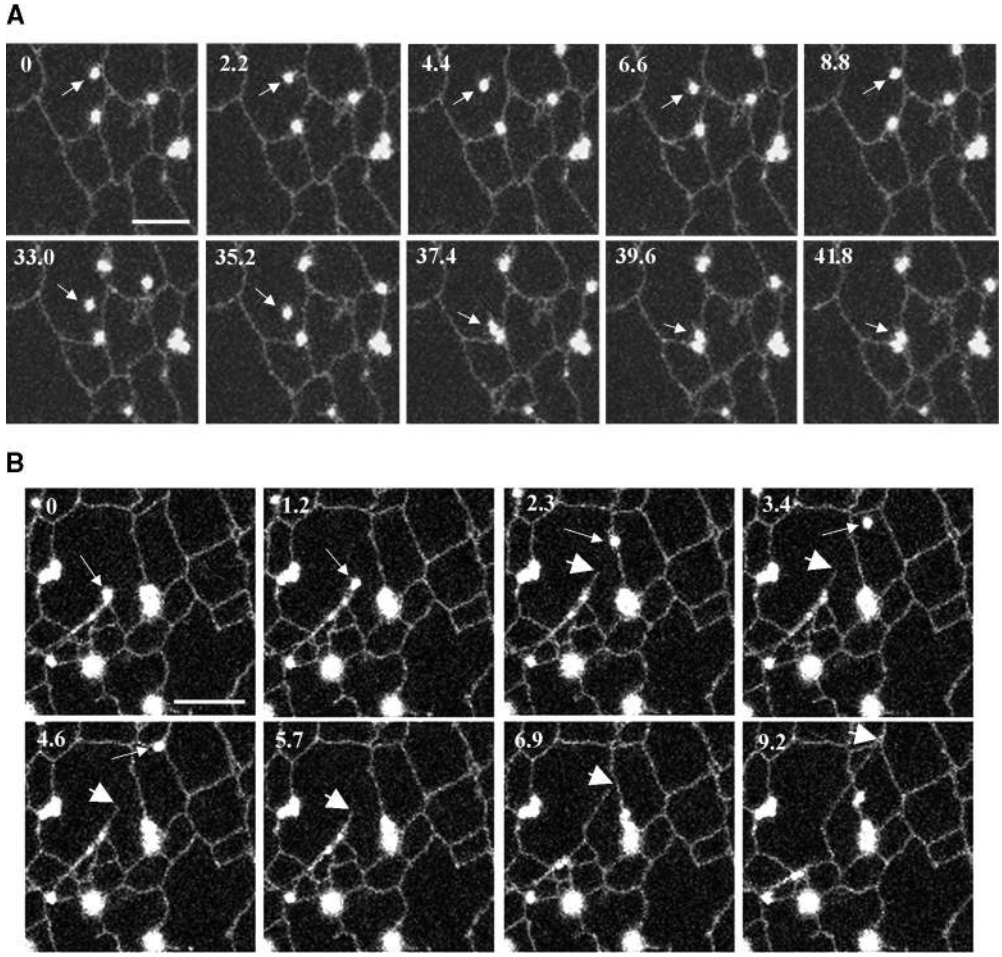

Figure 2. Time Lapse of an AtERD2-GFP Expressed in a *N. clevelandii* Leaf Trichome by Virus-Mediated Transient Expression.

(A) A Golgi body can be seen breaking free from the ER (arrows). A tubular membrane, probably originating from the ER, is visible (arrows in bottom row).

(B) A Golgi body (small arrows) appears to drag the ER tubules (large arrows) along the same trajectory.

Time is expressed in seconds at the top left of each frame. Bars = 5 μm.

stacks was found to arise under these conditions, with the heaviest stain at the forming (*cis*) face and weakest stain at the maturing (*trans*) face (Juniper et al., 1982). In face view, cisternae toward the *cis* face in epidermal leaf cells showed fenestrated margins from which thin tubular extensions emanated (Figure 3A). These tubules appeared to be in close contact with the ER (Figure 3A). In the more traditional cross-sectional view, direct connections between ER and Golgi cisternae toward the *cis* face of the stacks was observed (Figures 3B to 3C, arrows). Whether such connections are permanent or transient remains to be established. Their existence, however, implies that protein traffic between these two organelles may not need to occur by vesicle carriers.

Actin-Dependent Movement of Golgi Bodies along the ER

Previous work has shown that in stained plant tissue, Golgi bodies are associated with actin based on their codistribution with rhodamine-phalloidin (Boevink et al., 1998; Saint-Jore et al., 2002). This observation, together with other work (Nebenführ et al., 1999), has suggested that actin plays an important role in directing the movements of Golgi bodies along the ER. Consistent with this notion, we used time-lapse imaging experiments of tobacco epidermal cells coexpressing GFP fused to the actin binding region of mouse talin (talin-GFP) and ST-YFP and found that Golgi bodies moved along actin cables (Figures 4A to 4D). Moreover,

Golgi bodies halted their movement upon the addition of actin-depolymerizing agents such as latrunculin B, which dispersed the talin-GFP into the cytoplasm (Figures 4E to 4H). In AtERD2-GFP–transformed cells, Golgi bodies halted on small islands of lamellar ER formed at the junctions of the ER tubules (Figures 5D to 5F).

Golgi bodies did not always coalign with cortical microtubules when ST-GFP and tubulin-GFP (Ueda et al., 1999) were coexpressed (Figures 4I to 4L), again confirming the results from immunolabeling studies of ST-GFP–expressing cells (Saint-Jore et al., 2002). Moreover, disruption of microtubules using colchicine had no effect on the distribution and movement of Golgi bodies (Figures 4M to 4P), indicating that Golgi movement was not dependent on microtubules, as shown previously (Satiat-Jeunemaitre et al., 1996b; Nebenführ et al., 1999).

Constitutive Cycling of Golgi Proteins in and out of Golgi Bodies

Our ability to stop the directional movement of Golgi structures by latrunculin B treatment allowed us to investigate the extent of protein cycling of ST-GFP and AtERD2-GFP in and out of Golgi bodies using photobleaching recovery techniques. In these experiments, we selectively photobleached a single Golgi body and then monitored recovery into the bleached structure over time. A significant recovery indicates that the bleached molecules are exchanging with fluorescent pools of the protein localized in other parts of the cell. A lack of significant recovery indicates that the fluorescent molecules are stably associated with the Golgi structure and not undergoing significant cycling. As shown in Figures 5A to 5F, both ST-GFP and AtERD2-GFP showed rapid recovery into a photobleached Golgi body in cells treated with latrunculin. In both cases, fluorescence recovered to 80 to 90% of the prebleach level within 5 min. These results indicate that neither ST-GFP nor AtERD2-GFP is stably associated with the Golgi complex. Instead, they undergo continuous movement in and out of Golgi structures, presumably using membrane transport pathways that connect the Golgi with the ER. The data further imply that the movement of Golgi bodies along the surface of the ER is not necessary for the delivery of proteins from the ER to the Golgi, as suggested in the vacuum cleaner model for secretory transport in plants (Boevink et al., 1998).

Previous work examining Golgi protein cycling between the Golgi and the ER in mammalian cells has indicated a role for microtubules in providing tracks for the transport of membrane-bound intermediates from the ER to the Golgi (Cole et al., 1996; Presley et al., 1997). The fact that Golgi elements are closely opposed to the ER in plant cells raises the possibility that microtubules may not be important for protein trafficking between the Golgi and the ER in these cells. Consistent with this possibility, we found that when microtubules were depolymerized with colchicine in latrunculin B–treated cells expressing AtERD2-GFP and ST-GFP, no change in the rate of recovery into a photobleached Golgi body was observed compared with that in latrunculin B–treated cells alone (Figures 5G to 5L and 6A). Thus, in plant cells, neither intact actin nor microtubule elements are necessary for the rapid membrane cycling of ST-GFP and AtERD2-GFP between the Golgi and the ER.

Proteins with Different Golgi Locations Cycle in and out of Golgi Bodies at Identical Rates

AtERD2-GFP and ST-GFP have been shown to localize to different regions within the Golgi stack. AtERD2-GFP (in the

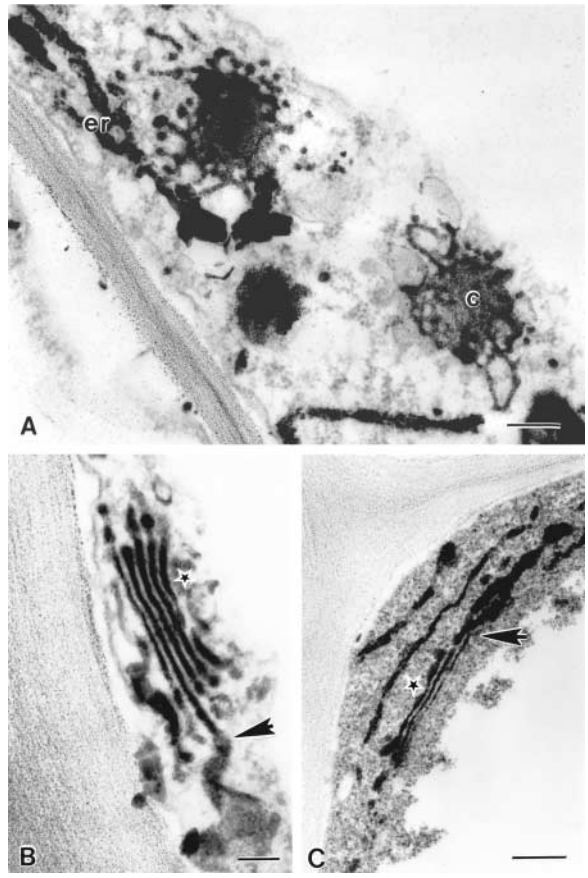

Figure 3. Electron Micrographs of Zinc Iodide– and Osmium Tetroxide–Impregnated Cells Show the Closeness of the Golgi and the ER.

(A) Conventional transmission electron micrograph of the ER (er) and the Golgi (G) after impregnation.
(B) and **(C)** Golgi stacks appear to have points in continuity with the ER (arrows). Star indicates the *trans* face of the Golgi.
Bars = 500 nm.

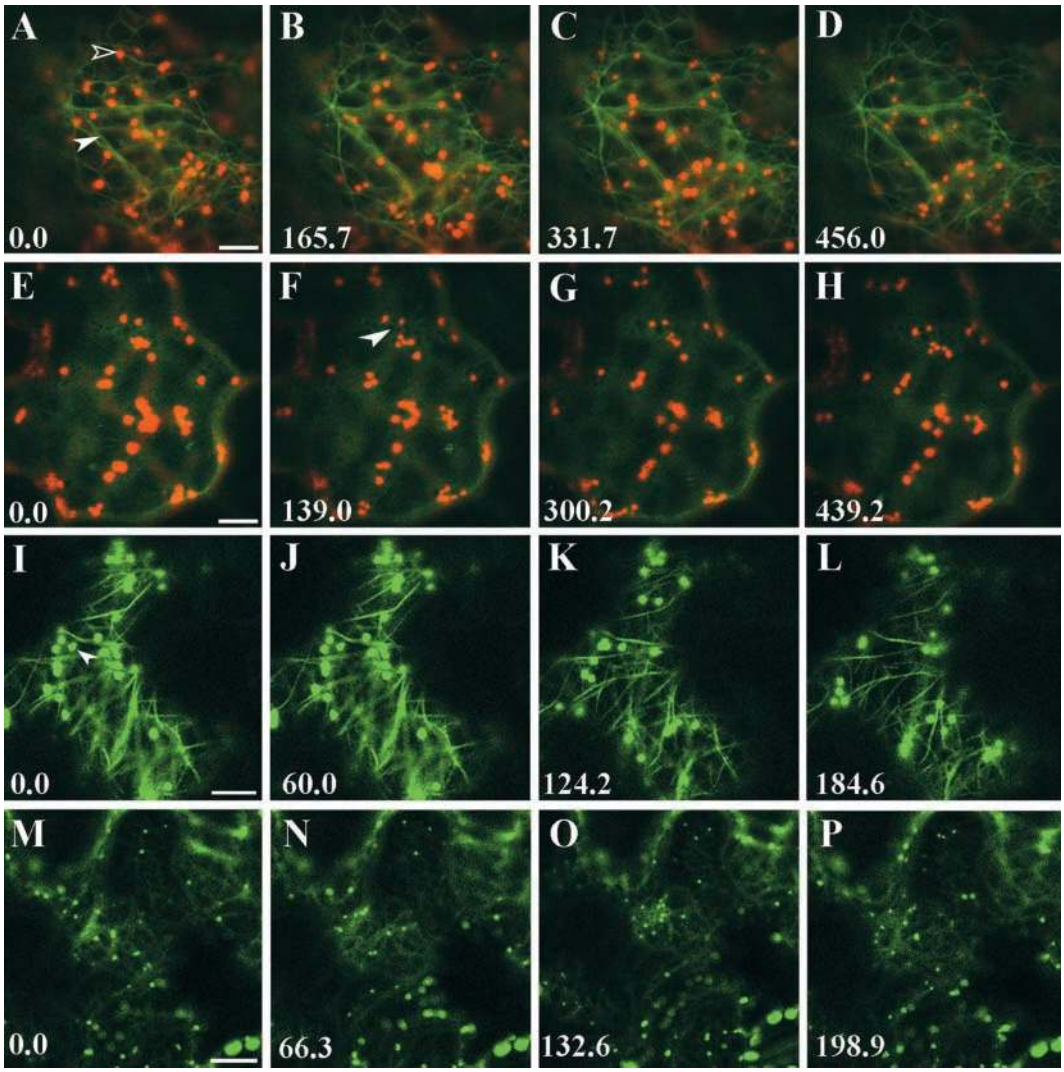

Figure 4. Golgi Stack Movement Requires the Actin Cytoskeleton and Occurs Independently of the Presence of Microtubules.

(A) to **(D)** Time lapse of a cell cotransformed with talin-GFP and ST-YFP. Golgi stacks (open arrowhead) align on actin cables (closed arrowhead). The actin network appears to be highly mobile. Bar = 5 μm.

(E) to **(H)** One hour of latrunculin B treatment (25 μM) induces actin depolymerization and cytoplasmic release of the talin-GFP construct. Cytoplasmic organelles are visible in negative contrast (**[F]**, arrowhead). Golgi movement is inhibited strongly after 1 h of latrunculin B treatment. Compare the time sequence **(A)** to **(D)** with **(E)** to **(F)** and note that the Golgi stacks in **(E)** to **(H)** are relatively immobile compared with those in **(A)** to **(D)** within similar time frames. Bar = 5 μm.

(I) to **(L)** Time lapse of an epidermal cell cotransformed with a tubulin-GFP construct and ST-GFP. Golgi stacks are mostly independent of the microtubule cytoskeleton (**[I]**, arrowhead). Bar = 5 μm.

(M) to **(P)** Depolymerization of microtubules with the drug colchicine does not prevent Golgi stacks from moving. This time series was taken after 1 h of treatment with 1 mM colchicine. Bar = 10 μm.

Time is expressed in seconds at the bottom left of each frame.

expression system of *Potato virus X*) localizes to all Golgi cisternae, whereas ST-GFP in this system or in Arabidopsis exhibits a greater concentration in *medial* and/or *trans* cisternae (Boevink et al., 1998; Wee et al., 1998). To determine whether proteins with different Golgi subdistributions have different Golgi residency times, we quantified the recovery rates after photobleaching individual Golgi bodies in latrunculin B–treated cells expressing AtERD2-GFP or ST-GFP (Figures 6A and 6B). No significant difference in the half-times for recovery was observed between these two proteins. This suggested

that the differences in steady state, intra-Golgi distribution of AtERD2-GFP and ST-GFP were not related to the speed of cycling of these proteins in and out of Golgi elements.

To determine if the rate of cycling of a Golgi protein is dependent on its glycosylation status, we photobleached Golgi bodies in cells expressing a glycosylated form of ST-GFP (ST-N-GFP; Batoko et al., 2000). ST-N-GFP differs from ST-GFP by the presence of 10 additional amino acids, including an *N*-glycosylatable Asn. The 3-kD increase in molecular mass of ST-N-GFP compared with ST-GFP confirms the presence of the Asn-linked carbohydrate chain on ST-N-GFP (data not shown). Despite this difference, ST-N-GFP exhibited the same recovery rate into a photobleached Golgi body in cells treated with latrunculin B to block Golgi movement (Figure 6A). Thus, whether a Golgi protein is glycosylated or not does not appear to affect its rate of cycling in and out of Golgi elements.

Effect of ATP Depletion and NEM on Golgi Protein Cycling

To begin to address the mechanistic basis for the rapid cycling of ST-GFP and AtERD2-GFP in and out of Golgi structures in plant cells, we examined the effect of ATP depletion and NEM treatment on this process. Both ATP depletion and NEM treatment have been shown previously to block protein trafficking between the Golgi and the ER (Orci et al., 1991). The basis for these effects is not understood entirely, but ATP depletion is thought to act by disrupting the assembly of membrane coat proteins (Aridor and Balch, 2000), whereas NEM (a protein Cys cross-linker) interferes with the activity of NEM-sensitive fusion protein, a homotrimer that mediates membrane fusion (Whiteheart et al., 1994). Within 40 min of treating transiently transformed epidermal cells with sodium azide and 2-deoxyglucose to deplete ATP levels, Golgi stacks stopped moving along the ER network. This phenomenon was reversible upon washout of the drugs and addition of Glc for 60 min (data not shown). When individual Golgi stacks labeled with AtERD2-GFP were photobleached in ATP-depleted cells, no fluorescence recovery was observed (Figures 6C and 7A to 7C).

NEM was found to inhibit Golgi movement within 10 min of treatment. Likewise, individual Golgi stacks labeled with AtERD2-GFP in NEM-treated cells (Figures 7D to 7F) did not recover after photobleaching. Similar results were observed for ST-GFP in fluorescence recovery after photobleaching experiments performed in ATP-depleted or NEM-treated cells (data not shown).

Effect of BFA on Golgi Protein Cycling

BFA is a fungal metabolite that in mammalian cells causes proteins of the COPI complex and ARF1 to dissociate from Golgi membranes and causes Golgi enzymes to redistribute into the ER (Donaldson et al., 1992). In plant cells, the effects of BFA are variable, and BFA molecular targets are still under discussion (Ritzenthaler et al., 2002; Saint-Jore et al., 2002). However, in many plant cells treated with BFA, Golgi proteins redistribute into the ER (Figures 8A and 8B).

To investigate the early effects of BFA on Golgi protein cycling in plant cells, we photobleached Golgi bodies labeled with ST-GFP and AtERD2-GFP in epidermal cells after the addition of BFA and before these proteins had redistributed into the ER (which occurs within 1 h of treatment). As in previous experiments, it was necessary to inhibit Golgi body movement with actin-depolymerizing agents before adding BFA. Strikingly, no fluorescence recovery into photobleached Golgi bodies labeled with AtERD2-GFP (Figures 8C to 8E) or ST-GFP (data not shown) was observed.

To confirm that the absence of recovery into the Golgi bodies was not caused by BFA-induced redistribution of the Golgi proteins into the ER during the recovery period, we simultaneously transformed epidermal cells with AtERD2-cyan fluorescent protein (CFP) and AtERD2-YFP or with ST-YFP and ST-CFP. We selectively photobleached YFP with the 514-nm laser line of the confocal microscope to follow the recovery of this fluorochrome and simultaneously imaged CFP for 5 to 10 min after bleaching. Cells cotransformed with AtERD2-CFP and AtERD2-YFP showed both labels in the same population of Golgi bodies. In cells treated with latrunculin B alone, photobleaching of YFP-labeled Golgi bodies was followed by the recovery of YFP fluorescence with no change in CFP fluorescence (Figures 8F to 8H). By contrast, in cells treated with latrunculin B and BFA, 40% of YFP-labeled Golgi bodies (100 Golgi stacks were sampled) that were bleached failed to recover despite the persistence of CFP labeling (Figures 8I to 8K). The same experimental procedure performed in cells expressing ST-CFP and ST-YFP showed a 50% recovery of 126 Golgi stacks sampled (Figures 8L to 8N). These results suggest that BFA can block transport into the Golgi of constitutively cycling Golgi proteins without blocking their retrograde transport back to the ER.

DISCUSSION

In this study, we investigated the dynamic aspects of the plant cell secretory pathway by the application of noninvasive fluorescence recovery after the use of photobleaching technology on GFP-labeled Golgi bodies.

Fluorescent Protein Constructs Confirm a Close Physical and Mechanical Relationship of the Golgi with the Actin Cytoskeleton but not with Microtubules in Vivo

Golgi bodies align with actin cables, as shown in epidermal cells coexpressing fluorescently labeled actin and Golgi

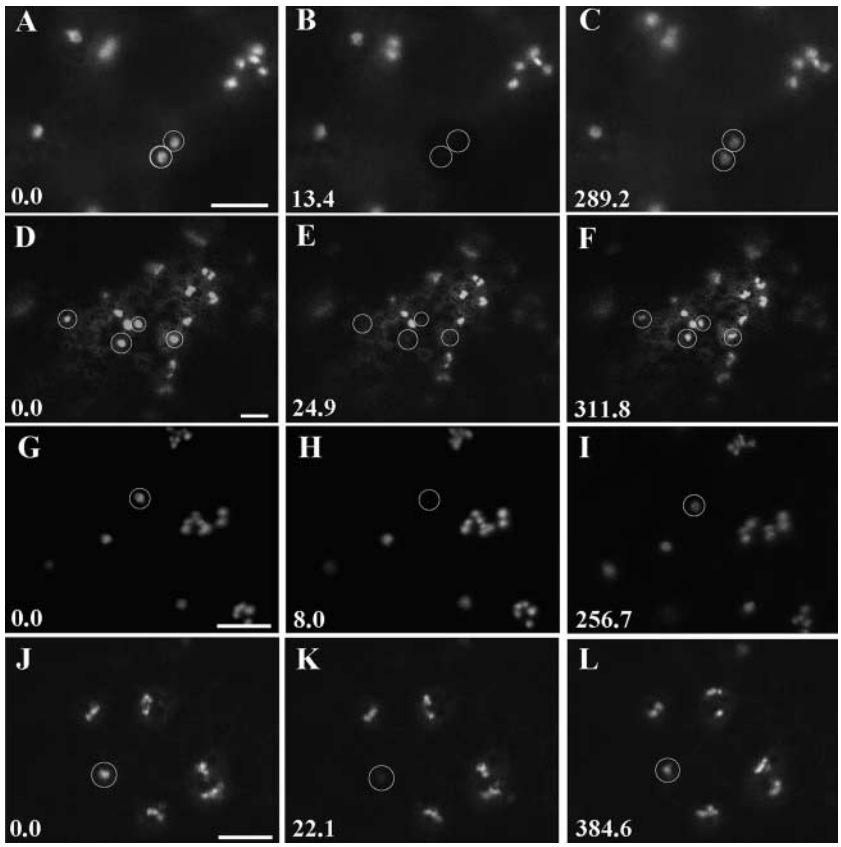

Figure 5. The Recovery of Fluorescence into Photobleached Golgi Stacks Does Not Require Actin or Microtubules.

(A) to **(C)** Two Golgi stacks (circles) labeled with ST-GFP **(A)** were photobleached **(B)** after treatment with the actin agent latrunculin B. After bleaching, the fluorescence recovered **(C)**.

(D) to **(F)** Four Golgi stacks in an AtERD2-GFP–transformed epidermal cell (**[D]**, circles) were photobleached **(E)** after latrunculin B treatment. Fluorescence recovered in the stacks **(F)**.

(G) to **(I)** ST-GFP Golgi in an epidermal cell (**[G]**, circle) treated with latrunculin B and the microtubule-depolymerizing agent colchicine **(I)** recovered after bleaching **(H)**.

(J) to **(L)** The fluorescence of AtERD2-GFP Golgi (**[J]**, circle) in latrunculin B– and colchicine-treated transformed epidermal cells **(L)** recovered after bleaching **(K)**.

Time is expressed in seconds at the bottom left of each frame. Bars = 5 μm.

bodies, confirming the result from fixed and rhodamine-phalloidin–stained GFP-expressing epidermal cells (Boevink et al., 1998). A similar labeling of actin in a range of plant tissues using GFP fused to the mouse talin actin binding site colocalizes exactly with the actin cytoskeleton, as revealed by rhodamine-phalloidin labeling, and is not detrimental to cell morphology or function (Kost et al., 1998). The in vivo leaf pattern was similar to that described previously in *N. clevelandii* epidermal cells that were virally transformed with AtERD2-GFP and labeled with rhodamine-phalloidin (Boevink et al., 1998). In our time-lapse experiment (Figures 4A to 4D), we showed that Golgi bodies not only align on, but also move over, the actin cables, as predicted by the previous use of actin-disrupting agents (Boevink et al., 1998; Nebenführ et al., 1999). Here, the actin-disrupting agents were found to release talin-GFP into the cytoplasm, consistent with the depolymerization of the actin cytoskeleton. Under these conditions, Golgi bodies stop their directional movement, demonstrating that Golgi movement is actin dependent, as reported previously (Boevink et al., 1998; Nebenführ et al., 1999). Moreover, the association of Golgi bodies with the ER is not actin dependent, because no ER-detached Golgi bodies are seen in the cytoplasm.

In epidermal cells expressing fluorescent tubulin and Golgi-targeted protein, Golgi stacks do not align tightly with microtubules as they do with actin, as shown by immuno-

cytochemistry on Bright Yellow 2 (BY2) cells (Saint-Jore et al., 2002). Moreover, disruption of the microtubule cytoskeleton does not inhibit Golgi directional movement, as reported for BY2 cells (Nebenführ et al., 1999). Thus, the organization of the plant endomembrane system differs significantly from that in animal cells, in which Golgi structures associate closely with microtubules rather than actin (Cole et al., 1996; Hawes et al., 1999).

Movement of the Golgi Is Not a Requirement for Membrane Protein Transport

Nicotiana leaf epidermal cells expressing AtERD2-GFP to label the ER and the Golgi showed Golgi stacks moving over the cortical ER network, as reported previously for GFP-Golgi proteins (Boevink et al., 1998). This is the most common situation; occasionally, however, Golgi bodies are seen to break free from the ER and may even drag behind them what appear to be short tails of ER (Figures 1C, 1D, and 2). Even then, Golgi bodies reassociate with ER strands. This close association of the ER with the Golgi apparatus suggests that the dynamics of ER modeling may be related closely to Golgi movement. High-resolution imaging of this movement showed that Golgi bodies moved in a stop-and-go manner. Interestingly, the Golgi stacks often were stationary at the three-way junctions of ER tubules. When we examined Golgi bodies in these cells by electron microscopy, we found that they were in close vicinity to the ER, which often showed what appeared to be direct continuity with Golgi stacks. This raised the possibility that Golgi bodies might continually receive cargo from the ER, irrespective of Golgi movement, and that this occurred via the ER in intimate and continual contact with individual Golgi stacks.

To test this possibility, we examined the effect of blocking Golgi movement on protein trafficking between the ER and the Golgi. In cells whose Golgi structures were immobile as a result of latrunculin B treatment, we found that AtERD2-GFP and ST-GFP showed no change in steady state distribution in the ER and the Golgi. More importantly, these proteins were found to undergo rapid cycling in and out of Golgi bodies. Evidence for this was obtained from photobleaching experiments. Selective photobleaching of a single Golgi body resulted in rapid fluorescence recovery. This occurs only if nonbleached molecules in the surrounding ER continually exchange bleached molecules in the Golgi, because photobleaching induces an irreversible loss of GFP fluorescence. Rapid fluorescence recovery was observed for all Golgi bodies that were photobleached, which indicates that cycling is not limited to a subset of Golgi structures but is a general property of all Golgi bodies.

These results show that the movement of Golgi stacks is not functionally coupled to protein trafficking between the ER and the Golgi in plant cells. However, we cannot exclude the possibility that the recovery of Golgi fluorescence would be faster during movement in the presence of an

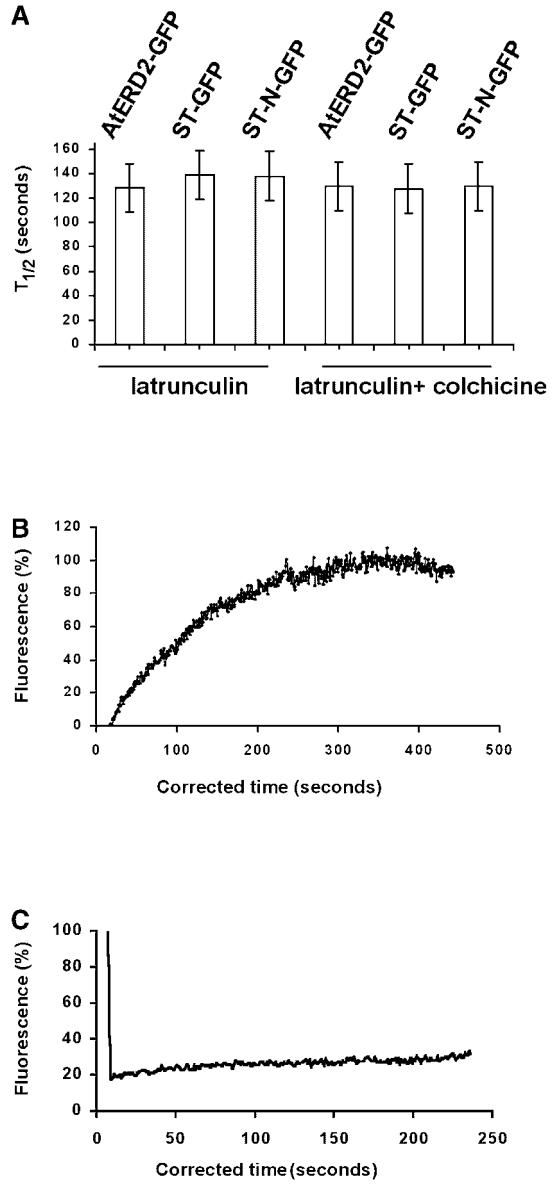

Figure 6. Fluorescence Half-Time Recoveries and Curves.

(A) The time of fluorescence recovery into photobleached Golgi stacks is similar in the absence of microtubules and/or actin for proteins with different locations in the Golgi and different glycosylation states. Data represent means ± SD ($n \geq 25$) and were significant at $P = 0.05$.

(B) Example of a half-time recovery plot. One hundred percent fluorescence indicates the prebleach fluorescence intensity.

(C) Representative fluorescence recovery curve of bleached Golgi in ATP-depleted cells expressed as a percentage of the initial fluorescence versus time.

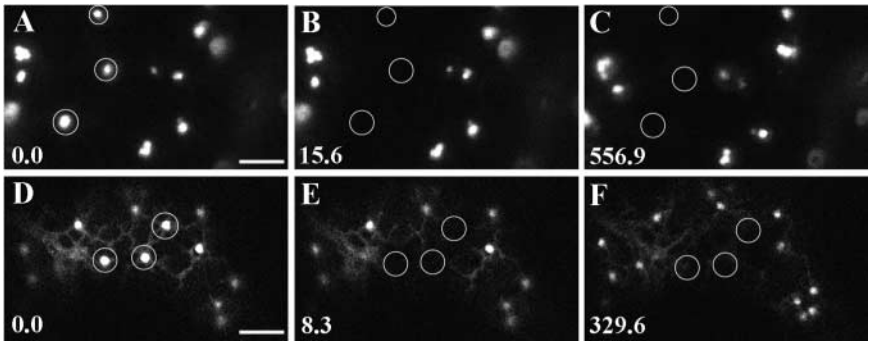

Figure 7. Recovery of Fluorescence into Photobleached Golgi Stacks Is ATP and Protein Dependent.

(A) to **(C)** Golgi stacks in an AtERD2-GFP–transformed epidermal cell. Golgi stacks (**[A]**, circles) were bleached **(B)**, and their fluorescence failed to recover in the presence of ATP depletors **(C)**.

(D) to **(F)** Golgi bodies (**[D]**, circles) were bleached **(E)** in a cell treated with the protein cross-linker NEM (20 mM) for 15 min. The fluorescence did not recover under these conditions **(F)**.

Time is expressed in seconds at the bottom left of each frame. Bars = 5 μm.

intact actin/microtubule cytoskeleton. Photobleaching experiments to precisely determine the cycling rate of GFP markers in cells that have not had their actin/microtubule cytoskeletons disrupted can confirm this, although it is difficult to monitor individual Golgi stacks under these conditions because they move so rapidly. In this view, the vacuum cleaner model for cargo transfer to the Golgi cannot be dismissed completely, because ER-to-Golgi protein transport may be more efficient during Golgi movement.

In the absence of the cytoskeleton, Golgi bodies may stop only on areas of the ER that have the capacity to export proteins (i.e., putative export sites). Similarly, the whole surface of the ER may be export competent, and the movement of ER membranes underneath the Golgi may be responsible for delivering cargo and membrane to the Golgi bodies. Another possibility is that both specialized ER export sites and Golgi stacks move together as one dynamic system, either through direct membrane continuities or through continuous membrane budding/fusion reactions. In this model, Golgi movement could be attributed to the need for cargo to be delivered throughout the plant cell.

The rapid AtERD2-GFP and ST-GFP cycling between the Golgi and the ER in latrunculin B–treated cells whose Golgi structures are immobile is likely to occur via specialized close connections between Golgi structures and nearby ER, rather than through random and continuous vesicle budding from the ER. This is because no vesicles or vesicle clouds enriched in GFP could be resolved in the cytoplasm as a result of the inhibition of Golgi motility. However, such "free" vesicles would be predicted to accumulate if vesicles carrying AtERD2-GFP to the Golgi normally bud from all over the ER (thereby requiring Golgi movement to "vacuum them up") or if they bud from stationary ER exit sites (thereby requiring Golgi stop-and-go movement to these sites).

The results of photobleaching experiments raise several questions concerning the nature of the residence time of membrane-bound proteins in the Golgi. Photobleaching induces the loss of fluorochrome activity but not the physical elimination of protein in the bleached organelle. Our fluorescence recovery after photocbleaching experiments suggest that proteins move continuously toward the Golgi. To maintain steady state fluorescence levels, there must be an equal continual loss of protein from the organelle, assuming that chimeric protein levels in the Golgi had reached a steady state at the start of each experiment. The protein loss could occur by retrograde membrane protein movement back toward the ER (i.e., recycling of Golgi components) and/or the loss of protein to other cellular destinations, such as the plasma membrane or the tonoplast. At this time, we cannot discriminate the two variants of the model (i.e., retrograde transport or outward transport). At the fluorescence level, we have not seen labeling of the plasma membrane or the vacuole. This movement cannot be excluded, however, considering that GFP may be degraded at the plasma membrane (Batoko et al., 2000) or the vacuole (Di Sansebastiano et al., 2001). Therefore, GFP accumulation may not be detected in these areas.

Recently, it was suggested that in mammalian cells, most of the Golgi machinery does recycle constitutively through the ER (Miles et al., 2001; Ward et al., 2001). One feature of this process must be the inability of transferases to function while in transient residence in the ER. In plants, it has been shown that HDEL/KDEL-containing glycoproteins remain endoglycosidase-H sensitive unless cells are treated with BFA (Frigerio et al., 2001; Saint-Jore et al., 2002). If proteins of the plant Golgi recycle to the ER, then the transferases must be either inactive or in residence for too short a time to function, or perhaps they recycle directly from export sites without mixing with lumenal proteins.

A final but less likely alternative explanation for such a rapid reestablishment of fluorescent proteins in the Golgi could be the possible degradation of proteins in the Golgi. However, we exclude this hypothesis on the basis that ST-GFP can reestablish Golgi fluorescence after BFA removal in the presence of protein synthesis inhibitors (Saint-Jore et al., 2002). This observation is not in agreement with a rapid degradation of the construct in the Golgi.

Energy and Protein Requirement to Accomplish Anterograde Transport of Membrane Proteins

It is assumed generally that soluble cargoes move from the ER to the Golgi in COPII-coated vesicles (Barlowe et al., 1994), and biochemical evidence has been presented recently in support of this mechanism in plants (Phillipson et al., 2001). However, some indication of COPII-independent transport in plants has been reported (Hara-Nishimura et al., 1998; Chrispeels and Herman, 2000; Toyooka et al., 2000; Törmäkangas et al., 2001). ER-to-Golgi transport of membrane proteins, such as ST-GFP and AtERD2-GFP, secretory, and vacuole-targeted forms of GFP, is compromised by the expression of nonfunctional Sar1p and AtRab1 mutants (Andreeva et al., 2000, Batoko et al., 2000, Takeuchi et al., 2000, Phillipson et al., 2001). Thus, in vivo evidence supports the idea that the COPII machinery, but not necessarily COPII vesicles, may be a prerequisite for exit from the ER.

The close spatial relationship between the ER and the Golgi in the leaf system raises the question of exactly how protein transport between the two organelles occurs. To determine the role of vesicle-related transport machinery, we performed photobleaching experiments to measure AtERD2-GFP and ST-GFP cycling in and out of Golgi structures in the presence of energy depletors or upon NEM treatment. Under conditions of energy depletion, as may be expected for a cytoskeletal motor-based system, the Golgi stacks stopped moving, but they regained motility when the energy depletors were removed. Similarly, transport from the ER to the Golgi depends on the availability of ATP, because photobleaching of Golgi bodies was not followed by the recovery of fluorescence. ATP may be required for a fundamental step in the transport process, such as the production of GTP for the putative GTPases involved in transport or for myosin motors, which could be involved in vesicle tethering and cargo delivery. Similarly, inhibition of the recovery of Golgi fluorescence after photobleaching AtERD2-GFP by NEM indicates some role of regulatory and or structural proteins in the process that presumably has an energy requirement.

BFA Restricts Anterograde Movement

In plants as in mammalian cells, it is well accepted that BFA inhibits secretion (Wood et al., 1991; Gomez and Chrispeels, 1993; Schindler et al., 1994; Boevink et al., 1999). In tobacco leaves, the fluorescence of Golgi bodies labeled with ST-GFP and AtERD2-GFP is redistributed into the ER in the presence of BFA (Boevink et al., 1998; Saint-Jore et al., 2002). A similar phenomenon has been reported in BY2 cells (Ritzenthaler et al., 2002; Saint-Jore et al., 2002), and it has been shown that this process is reversible and not dependent on the cytoskeleton (Saint-Jore et al., 2002). BFA also has been shown to induce the formation of vesicular "BFA compartments," as observed by electron microscopy (Satiat-Jeunemaitre et al., 1996a), large fluorescent aggregates in GFP-expressing systems (Baldwin et al., 2001), and ER-Golgi hybrid stacks (Ritzenthaler et al., 2002).

In animal cells, a structural disruption of Golgi integrity occurs upon BFA treatment, causing extensive tubulation and redistribution of Golgi membrane (Lippincott-Schwartz et al., 1990) and most other protein components (Ward et al., 2001) to the ER. However, it has been suggested that protein components of the Golgi, which constitute the matrix and structural scaffold of this organelle, may remain in the cytoplasm (Seemann et al., 2000). The exact mechanism by which secretion is inhibited in plants is unknown, causing considerable controversy about the sites of action of BFA, which could be linked to the hypothesized multiple BFA binding sites in plant cells (Staehelin and Driouich, 1997). However, it is clear that one initial effect in BY2 cells is the loss of ARF1 and γCOP from the Golgi, presumably inhibiting the formation of Golgi-associated COPI vesicles, as in mammalian cells, before the formation of an ER-Golgi hybrid compartment (Ritzenthaler et al., 2002). Thus, it is possible that secretion stops as the Golgi membranes disappear after incorporation into the ER, although other mechanisms cannot be excluded, such as an interruption of ER-to-Golgi transport.

To investigate the effect of BFA on ER/Golgi trafficking in plant cells in vivo, we selectively bleached Golgi stacks labeled with YFP and followed the integrity of the membranes by simultaneous observation of a similar CFP construct labeling the same stack. When AtERD2-YFP or ST-YFP was bleached in the presence of BFA after 10 min of treatment, but before the redistribution of fluorescence into the ER, no recovery of fluorescence was observed in 50% (ST-YFP) and 40% (AtERD2-YFP) of labeled stacks. During the recovery period, the CFP signal indicated that photobleaching does not damage the Golgi at the resolution offered by confocal imaging. Moreover, the double-expression results indicate that BFA treatment can inhibit forward transport to the Golgi before a detectable (within the limits of light microscopy) morphological change in the Golgi and Golgi membrane reabsorption into the ER can occur.

Rapid loss of the COPI coat from Golgi membranes as a result of BFA inhibition of the ARF1 guanine nucleotide exchange factor (Robineau et al., 2000; Ritzenthaler et al., 2002) provides a reasonable explanation for how forward trafficking could be affected by BFA. In mammalian cells, BFA treatment has been shown to prevent Golgi enzymes

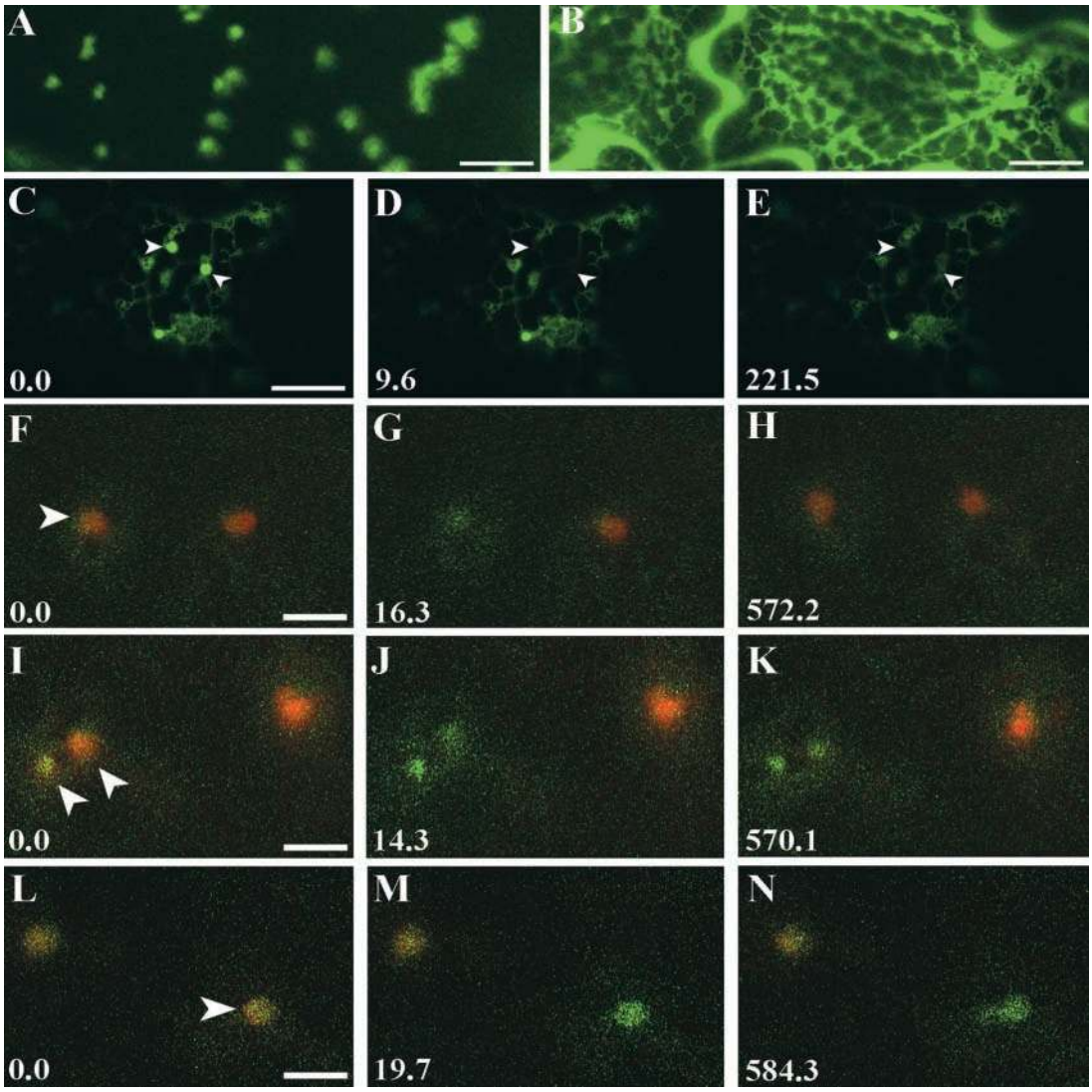

Figure 8. Analysis of the Effect of the Secretory Inhibitor BFA.

(A) Golgi stacks in an epidermal cell transformed with ST-GFP.
(B) Addition of BFA causes reabsorption of the Golgi membranes in the ER within 1 h of treatment.
(C) and **(D)** Photobleaching **(D)** of Golgi stacks (**[C]**, arrowheads) in an AtERD2-transformed epidermal cell treated with cytochalasin D (20 μg/mL for 30 min) and BFA. No fluorescence was recovered by 220 s after bleaching. The bleaching experiment started at 20 min after the addition of BFA **(E)**. Bar = 5 μm.
(F) to **(H)** Golgi (**[F]**, arrowhead) of epidermal cells treated with latrunculin cotransformed with AtERD2-CFP (green) and AtERD2-YFP (red) were photobleached of the YFP fluorescence **(G)**. Fluorescence recovery was observed **(H)**. Bar = 2 μm.
(I) to **(K)** Fluorescence of photobleached **(J)** AtERD2-YFP Golgi stacks (**[I]**, arrowheads) in cells treated with latrunculin and BFA did not recover **(K)**. The bleaching experiment started at 30 min after the addition of BFA. Bar = 2 μm.
(L) to **(N)** Photobleached **(M)** ST-YFP Golgi (**[L]**, arrowhead) in epidermal cells cotransformed with ST-CFP (green) in the presence of latrunculin and BFA did not recover **(N)**. The bleaching experiment started at 25 min after the addition of BFA. Bar = 2 μm.
Time is expressed in seconds at the bottom left of each frame.

and soluble cargo from being recruited to ER exit sites, even though the Sar1-COPII system remains operational at these sites (Ward et al., 2001). This finding has led to the proposal that the sequential activity of the Sar1-COPII and ARF1-coatomer systems serves to form and maintain Golgi structures, whose components circulate continuously through the ER (Ward et al., 2001). In this view, ARF1-coatomer is required for forward trafficking out of the ER because of its role in differentiating ER exit domains formed by the Sar1-COPII system. Without the joint activities of both Sar1-COPII and ARF1-coatomer, forward trafficking into the Golgi cannot occur. Our finding in plant cells that BFA blocks the transport of AtERD2-GFP and ST-GFP to the Golgi provides important support for this model.

On the Relationship between the ER and the Golgi

Based on the results reported above, the Golgi and the adjacent ER appear to serve as mobile functional secretory units in leaf cells, with both the Golgi and its associated ER undergoing continuous membrane cycling. The actin-based movement of these secretory units presumably would ensure that plant cells deliver cargo efficiently to diverse locations within the cell. How such differentiated ER-Golgi membrane units arise and are maintained in leaves is an important area for future investigation. In mammalian cells, similarly appearing Golgi ministacks in close association with transitional ER exit sites (Cole et al., 1996) arise in cells treated with nocodazole to disrupt microtubules.

The basis for the formation of Golgi ministacks in mammalian cells is that microtubule disruption inhibits the movement of pre-Golgi structures into the Golgi region (Presley et al., 1997). Redistribution of the Golgi membrane occurs under these conditions because Golgi components undergo continuous cycling through the ER (Storrie and Yang, 1998; Zaal et al., 1999; Ward et al., 2001) and reform Golgi structure at any site where membrane transport is inhibited or blocked (Cole et al., 1996). In leaves, Golgi membranes do not interact with microtubules. Disassembly of the actin cytoskeleton does not impair the rapid cycling of proteins in and out of the Golgi or the integrity of the stacks and does not induce the detachment of Golgi bodies from the ER. Whether this remarkable similarity between plant Golgi and mammalian ministacks reflects an underlying homology between mechanisms for stack formation and integrity has yet to be determined.

COPII machinery, which mediates ER export (Barlowe et al., 1994), has been shown in plants to be required for the ER-to-Golgi transport of membrane proteins, such as ST-GFP and AtERD2-GFP, secretory, and vacuole-targeted forms of GFP (Andreeva et al., 2000, Batoko et al., 2000, Takeuchi et al., 2000). Because this machinery is highly enriched in the ER domains in the vicinity of Golgi ministacks in microtubule-disrupted mammalian cells (Ward et al., 2001), COPII also might be enriched in the ER domains adjacent to Golgi stacks in plants. We are testing this hypothesis in our laboratory at present.

In conclusion, we have found that in tobacco leaves, Golgi bodies appear to be associated intimately with the cortical ER (Boevink et al., 1998). This is the case as well in other species, such as Arabidopsis (C.M. Saint-Jore, I. Moore, and C. Hawes, unpublished data). On the basis of transmission electron microscopy analysis, it appears that direct connections of the Golgi with the ER may exist (Figure 3), as reported previously in other systems (Juniper et al., 1982; Harris and Oparka, 1983), although at present we cannot establish whether these connections are permanent or transient. Our results from photobleaching experiments, which allowed us to study protein trafficking between the ER and the Golgi, have revealed that despite the apparent continuity between these organelles, protein transfer between them is dependent on BFA- and NEM-sensitive factors and is energy dependent. These findings, together with others in the plant field showing roles of Rab1p, Sar1p, and Sec12p (Batoko et al., 2000; Takeuchi et al., 2000; Phillipson et al., 2001) in protein traffic, implies that the same machinery that regulates secretory trafficking in animal cells is used in plant cells. Future work in this field likely will be aimed at understanding the basis for the unique features of the plant ER-Golgi system, including its rapid movement along actin cables and its relationship to ER remodeling.

METHODS

Molecular Cloning

Standard molecular techniques were used as described in Sambrook et al. (1989). For *Agrobacterium tumefaciens* transient expression, we used the binary vector pVKH18-EN6 (Batoko et al., 2000). To generate the ST-YFP, ST-CFP, AtERD2-YFP, and AtERD2-CFP constructs, mGFP5 (Haseloff et al., 1997) of the pVKH18-EN6::ST-GFP and pVKH18-EN6::AtERD2-GFP constructs (Saint-Jore et al., 2002) was substituted for by the enhanced yellow fluorescent protein (YFP) and cyan fluorescent protein (CFP) sequences from Clontech (Palo Alto, CA), using the unique SalI and SacI sites at the 5′ and 3′ ends of GFP5, respectively. The actin binding domain of mouse talin (Kost et al., 1998) was amplified by reverse transcriptase from total RNA using primer FB144 (5′-TTAGTGCTCGTCTCGAAGCTCTG-3′). The product then was amplified by PCR using TaqVent polymerase (New England Biolabs, Hitchin, UK) with primer FB144 in combination with FB143 (5′-CAAATCCTAGAAGCTGCCAAGTCC-3′).

The resulting product then was reamplified using the Taq/Pwo polymerase (Hybaid, Ashford, UK) with primer FB150 (5′-GGTGCTGGATCCGGTGCCGGCGCTGGCATCCTAGAAGCTGCCAAGTCCATCGC-3′) containing a BamHI site and three Gly and two Ala residues before the coding region of the protein and primer FB146 (5′-GCGCCGGAGCTCTTAGTGCTCGTCTCGAAGCTCTG-3′) containing a SacI site and a stop codon. The PCR product then was cloned in frame downstream of GFP5 into a pVKH18-EN6 binary vector. The resulting fusion protein contained a spacer between the

green fluorescent protein (GFP) and the cloned actin binding site of the mouse talin consisting of the following amino acids: GAG-SGAGAG.

Plant Material and Transient Expression Systems

Four-week-old tobacco (*Nicotiana tabacum* SR1 cv Petit Havana) greenhouse plants grown at 21°C were used for Agrobacterium-mediated transient expression (Batoko et al., 2000). Briefly, each expression vector was introduced into *Agrobacterium* strain GV3101 (pMP90) by heat shock. A single colony from the transformants was inoculated into 5 mL of YEB medium (per liter: 5 g of beef extract, 1 g of yeast extract, 5 g of Suc, and 0.5 g of $MgSO_4 \cdot 7H_2O$) supplemented with 100 μg/mL kanamycin. The bacterial culture was incubated at 30°C with agitation for 20 h. One milliliter of bacterial culture then was pelleted in an Eppendorf tube by centrifugation at 2200*g* for 5 min at room temperature. The pellet was washed once with 1 mL of infiltration medium (50 mM Mes, 2 mM $Na_3PO_4 \cdot 12H_2O$, 1 mM acetosyringone, and 5 mg/mL Glc) and then resuspended in 1 mL of the same buffer. For experiments requiring coexpression of two different constructs, 0.5 mL of each bacterial culture was mixed before washing in infiltration medium.

The bacterial suspension was inoculated using a 1-mL syringe without a needle by gentle pressure through the stomata on the lower epidermal surface. Transformed plants then were incubated under normal growth conditions. Where indicated, the expression system of *Potato virus X* was used to transform *Nicotiana clevelandii* plants as described previously (Boevink et al., 1998).

Drug Treatments

Segments of transformed leaves (~5 mm^2) were used for drug treatment, confocal imaging, and analysis. For actin depolymerization, leaf tissue was submerged in 25 μM latrunculin B (Calbiochem; stock solution, 10 mM in DMSO) for 1 h. Alternatively, 20 μg/mL cytochalasin D (Sigma-Aldrich; stock solution, 1 mg/mL in DMSO) was used for at least 30 min.

For microtubule depolymerization, leaf tissue was submerged in 1 mM colchicine (Sigma-Aldrich; stock solution, 100 mM in H_2O) for at least 30 min. After 30 min of treatment, tubulin-GFP fluorescence already was distributed in the cytoplasm. For actin and microtubule cytoskeleton depolymerization, leaf tissue was submerged in latrunculin B (25 μM) for 30 min. This was followed by treatment with a solution containing both latrunculin (25 μM) and colchicine (1 mM) for another 30 min before mounting the sample in this last solution for confocal analysis.

The protein cross-linker *N*-ethylmaleimide (Sigma-Aldrich; stock solution, 1 M in DMSO) was used at a concentration of 20 to 50 mM for at least 10 min before analysis. Brefeldin A (BFA) (Sigma-Aldrich; stock solution, 10 mg/mL in DMSO) was used at a concentration of 100 μg/mL. In our experience, this concentration is suitable to achieve a rapid reabsorption of most of the Golgi bodies into the endoplasmic reticulum in leaf epidermal cells. To follow BFA's effect on Golgi reabsorption to the endoplasmic reticulum, leaf tissue was dipped in BFA for 10 min and then mounted on a microscope slide for confocal observations.

For photobleaching experiments with BFA, segments of tissue were pretreated for 1 h with latrunculin B (or for 30 min with 20 μg/mL cytochalasin D) as described above to stop Golgi movement. Leaf segments then were immersed in a solution containing 25 μM latrunculin B (or 20 μg/mL cytochalasin D) and 100 μg/mL BFA. After 10 min, samples were mounted on a slide for selective photobleaching experiments. These were performed within 1 h of the addition of BFA.

For energy-depletion experiments, leaf tissue was submerged for at least 40 min in a solution containing both 50 mM 2-deoxyglucose (Sigma-Aldrich; stock solution, 1 M in H_2O) and 0.02% sodium azide (Sigma-Aldrich; stock solution, 2% in H_2O). To achieve recovery from ATP depletors, three washes of 5 min each were performed, submerging the tissue in H_2O. This was followed by the immersion of the tissue in 50 mM Glc for 1 h (British Drug House; stock solution, 1 M in H_2O).

All stock solutions were kept at −20°C, and working solutions were prepared fresh just before use. For analysis and observation at the microscope, samples were mounted on a slide with the solution in which they were last treated. When drugs were not used, segments of tissue were mounted in water.

Sampling and Imaging

Transformed leaves were analyzed at 72 h after infection of lower epidermal cells. Confocal imaging was performed using an inverted Zeiss LSM 510 laser scanning microscope and a ×40 oil immersion objective (Jena, Germany).

For imaging expression of GFP constructs, excitation lines of an argon ion laser of 488 nm were used with a 505/530-nm bandpass filter in the single-track facility of the microscope. For imaging coexpression of YFP and GFP constructs, excitation lines of an argon ion laser of 458 nm for GFP and 514 nm for YFP were used alternately with line switching using the multi-track facility of the microscope. Fluorescence was detected using a 458/514-nm dichroic beam splitter and a 475/525-nm bandpass filter for GFP and a 560/615-nm bandpass filter for YFP.

For imaging coexpression of CFP and YFP constructs, excitation lines of an argon ion laser of 458 nm for CFP and 514 nm for YFP were used alternately with line switching using the multi-track facility of the microscope. Fluorescence was detected using a 458/514-nm dichroic beam splitter with 570-nm and 515-nm dichroic filters and a 475- to 525-nm bandpass filter for CFP and a 530-590IR nm bandpass filter for YFP. In this way, any cross-talk and bleed-through of fluorescence were eliminated. Time-lapse scanning was performed with Zeiss LSM 510 imaging system software. Postacquisition image processing was with the LSM 5 Image Browser (Zeiss) and Adobe Photoshop 5.0 software (Mountain View, CA).

Photobleaching Recovery Studies

Spot photobleaching recovery measurements were performed on an inverted Zeiss confocal laser scanning microscope 510. A ×40 oil immersion objective lens was used. Zeiss software was used to record prebleach and postbleach signals and to modulate laser beam intensity. For quantification of fluorescence, signals were sampled before bleach treatment (generally, 10 data points) and >10 min after bleach treatment with low-intensity illumination (generally, 1 to 5% transmittance). Fluorescence of selected regions was bleached by scanning with high-intensity illumination (100% transmittance; Nehls et al., 2000).

For all experiments, the size of the bleached region of interest was 8.5 μm^2. Imaging conditions for all experiments were determined by experiments performed on AtERD2-GFP–expressing cells fixed with

paraformaldehyde to obtain no significant bleaching of the whole cell during the course of the experiment. The half-time ($t_{1/2}$) was the time required for fluorescence in the photobleached region to recover to 50% of the recovery asymptote. The $t_{1/2}$ in fluorescence recovery after photobleaching experiments was determined by scaling the postbleach fluorescence recovery to a 0 to 100% scale with the immediate postbleach intensity being 0% and the asymptote of the recovery being 100%. Time was rescaled with time 0 being equal to the $t_{1/2}$ of the photobleach, as described by Ellenberg et al. (1997). Significance statistics were determined using Student's two-tailed *t* test for two samples assuming equal variance.

Electron Microscopy

Segments of leaves from *N. clevelandii* and tobacco plants were fixed in 1% paraformaldehyde and 1% glutaraldehyde in 0.1 M sodium cacodylate buffer for 40 to 60 min and impregnated in a freshly made mixture of zinc iodide and osmium tetroxide (Hawes et al., 1981), dehydrated in a graded water-ethanol series, and embedded in Spurr's resin. After thin sectioning and contrasting with lead citrate, micrographs were taken with a JEOL 1200EXII transmission electron microscope.

ACKNOWLEDGMENTS

Sophie Marc Martin and Nadine Paris (Laboratoire de Biochimie, Neuchâtel, Switzerland) prepared the pVKH18-EN6::ST-YFP, ST-CFP, AtERD2-YFP, and AtERD2-CFP constructs. The tubulin-GFP construct was a kind gift of T. Hashimoto (Nara Institute of Science and Technology, Nara, Japan), and ST-N-GFP was a gift from H. Batoko (Oxford University, Oxford, UK). A. Andreeva (School of Biological and Molecular Sciences, Oxford Brookes University) prepared *N. clevelandii* leaf material for electron microscopy. F.B. was supported by a Biotechnology and Biological Sciences Research Council grant to C.H. E.S. is supported by the Pharmacology Research Associate Program.

Received January 15, 2002; accepted March 1, 2002.

REFERENCES

Andreeva, A.V., Kutuzov, M.A., Evans, D.E., and Hawes, C.R. (1997). Rab-GDP dissociation inhibitor isoforms in *Arabidopsis thaliana*. J. Exp. Bot. **48,** 2109–2110.

Andreeva, A.V., Zheng, H., Saint-Jore, C.M., Kutuzov, M.A., Evans, D.E., and Hawes, C.R. (2000). Organization of transport from endoplasmic reticulum to Golgi in higher plant. Biochem. Soc. Trans. **28,** 505–512.

Aridor, M., and Balch, W.E. (2000). Kinase signaling initiates coat complex II (COPII) recruitment and export from the mammalian endoplasmic reticulum. J. Biol. Chem. **275,** 35673–35676.

Baldwin, T.C., Handford, M.G., Yuseff, M.-I., Orellana, A., and Dupree, P. (2001). Identification and characterization of GONST1, a Golgi-localized GDP-mannose transporter in Arabidopsis. Plant Cell **13,** 2283–2295.

Barlowe, C. (2000). Traffic COPs of the early secretory pathway. Traffic **1,** 371–377.

Barlowe, C., Orci, L., Yeung, T., Hosobuchi, M., Hamamoto, S., Salama, N., Rexach, M.F., Ravazzola, M., Amherdt, M., and Schekman, R. (1994). COPII: A membrane coat formed by sec proteins that drive vesicle budding from the endoplasmic reticulum. Cell **77,** 895–907.

Batoko, H., Zheng, H.Q., Hawes, C., and Moore, I. (2000). A Rab1 GTPase is required for transport between the endoplasmic reticulum and Golgi apparatus and for normal Golgi movement in plants. Plant Cell **12,** 2201–2217.

Boevink, P., Martin, B., Oparka, K., Cruz, S.S., and Hawes, C. (1999). Transport of virally expressed green fluorescent protein through the secretory pathway in tobacco leaves is inhibited by cold shock and brefeldin A. Planta **208,** 392–400.

Boevink, P., Oparka, K., Santa-Cruz, S., Martin, B., Betteridge, A., and Hawes, C. (1998). Stacks on tracks: The plant Golgi apparatus traffics on an actin/ER network. Plant J. **15,** 441–447.

Chrispeels, M.J., and Herman, E.M. (2000). Endoplasmic reticulum-derived compartments function in storage and as mediators of vacuolar remodeling via a new type of organelle, precursor protease vesicles. Plant Physiol. **123,** 1227–1233.

Cole, N.B., Sciaky, N., Marotta, A., Song, J., and Lippincott-Schwartz, J. (1996). Golgi dispersal during microtubule disruption: Regeneration of Golgi stacks at peripheral endoplasmic reticulum exit sites. Mol. Biol. Cell **7,** 631–650.

Di Sansebastiano, G.P., Paris, N., Marc-Martin, S., and Neuhaus, J.M. (2001). Regeneration of a lytic central vacuole and of neutral peripheral vacuoles can be visualized by green fluorescent proteins targeted to either type of vacuoles. Plant Physiol. **126,** 78–86.

Donaldson, J.G., Finazzi, D., and Klausner, R.D. (1992). Brefeldin-A inhibits Golgi membrane-catalyzed exchange of guanine-nucleotide onto ARF protein. Nature **360,** 350–352.

Ellenberg, J., Siggia, E.D., Moreira, J.E., Smith, C.L., Presley, J.F., Worman, H.J., and Lippincott-Schwartz, J. (1997). Nuclear membrane dynamics and reassembly in living cells: Targeting of an inner nuclear membrane protein in interphase and mitosis. J. Cell Biol. **138,** 1193–1206.

Frigerio, L., Pastres, A., Prada, A., and Vitale, A. (2001). Influence of KDEL on the fate of trimeric or assembly-defective phaseolin: Selective use of an alternative route to vacuoles. Plant Cell **13,** 1109–1126.

Gomez, L., and Chrispeels, M.J. (1993). Tonoplast and soluble vacuolar proteins are targeted by different mechanisms. Plant Cell **5,** 1113–1124.

Hammond, A.T., and Glick, B.S. (2000). Dynamics of transitional endoplasmic reticulum sites in vertebrate cells. Mol. Biol. Cell **11,** 3013–3030.

Hara-Nishimura, I., Shimada, T., Hatano, K., Takeuchi, Y., and Nishimura, M. (1998). Transport of storage proteins to protein storage vacuoles is mediated by large precursor-accumulating vesicles. Plant Cell **10,** 825–836.

Harris, N., and Oparka, K. (1983). Connections between dictyosomes, ER and GERL in cotyledons of mung bean (*Vigna radiata* L.). Protoplasma **114,** 93–102.

Haseloff, J., Siemering, K.R., Prasher, D.C., and Hodge, S. (1997). Removal of a cryptic intron and subcellular localization of green fluorescent protein are required to mark transgenic Arabidopsis plants brightly. Proc. Natl. Acad. Sci. USA **94,** 2122–2127.

Hawes, C., Saint-Jore, C.M., Brandizzi, F., Zheng, H.Q., Andreeva,

A.V., and Boevink, P. (2001). Cytoplasmic illuminations: In planta targeting of fluorescent proteins to cellular organelles. Protoplasma **215,** 77–88.

Hawes, C.R., Brandizzi, F., and Andreeva, A.V. (1999). Endomembranes and vesicle trafficking. Curr. Opin. Plant Biol. **2,** 454–461.

Hawes, C.R., Juniper, B.E., and Horne, J.C. (1981). Low and high voltage electron microscopy of mitosis and cytokinesis in maize roots. Planta **152,** 397–407.

Juniper, B.E., Hawes, C.R., and Horne, J.C. (1982). The relationships between the dictyosomes and the forms of endoplasmic reticulum in plant cells with different export programmes. Bot. Gaz. **143,** 135–145.

Kost, B., Spielhofer, P., and Chua, N.-H. (1998). A GFP-mouse talin fusion protein labels plant actin filaments *in vivo* and visualises the actin cytoskeleton in growing pollen tubes. Plant J. **16,** 393–401.

Ladha, S., Mackie, A.R., Harvey, L.J., Clark, D.C., Lea, E.J.A., Brullemans, M., and Duclohier, H. (1996). Lateral diffusion in planar lipid bilayers: A fluorescence recovery after photobleaching investigation of its modulation by lipid composition, cholesterol, or alamethicin content and divalent cations. Biophys. J. **71,** 1364–1373.

Lippincott-Schwartz, J., Donaldson, J.G., Schweizer, A., Berger, E.G., Hauri, H.P., Yuan, L.C., and Klausner, R.D. (1990). Microtubule-dependent retrograde transport of proteins into the ER in the presence of brefeldin-A suggests an ER recycling pathway. Cell **60,** 821–836.

Lippincott-Schwartz, J., Roberts, T.H., and Hirschberg, K. (2000). Secretory protein trafficking and organelle dynamics in living cells. Annu. Rev. Cell Dev. Biol. **16,** 557–589.

Lippincott-Schwartz, J., Snapp, E., and Kenworthy, A. (2001). Studying protein dynamics in living cells. Nat. Rev. Mol. Cell Biol. **2,** 444–456.

Miles, S., McManus, H., Forsten, K.E., and Storrie, B. (2001). Evidence that the entire Golgi apparatus cycles in interphase HeLa cells: Sensitivity of Golgi matrix proteins to an ER exit block. J. Cell Biol. **155,** 543–555.

Nebenführ, A., Gallagher, L.A., Dunahay, T.G., Frohlick, J.A., Mazurkiewicz, A.M., Meehl, J.B., and Staehelin, L.A. (1999). Stop-and-go movements of plant Golgi stacks are mediated by the acto-myosin system. Plant Physiol. **121,** 1127–1142.

Nehls, S., Snapp, E.L., Cole, N.B., Zaal, K.J.M., Kenworthy, A.K., Roberts, T.H., Ellenberg, J., Presley, J.F., Siggia, E., and Lippincott-Schwartz, J. (2000). Dynamics and retention of misfolded proteins in native ER membranes. Nat. Cell Biol. **2,** 288–295.

Orci, L., Tagaya, M., Amherdt, M., Perrelet, A., Donaldson, J.G., Lippincott-Schwartz, J., Klausner, R.D., and Rothman, J.E. (1991). Brefeldin-A, a drug that blocks secretion, prevents the assembly of non-clathrin-coated buds on Golgi cisternae. Cell **64,** 1183–1195.

Phillipson, B.A., Pimpl, P., daSilva, L.L.P., Crofts, A.J., Taylor, J.P., Movafeghi, A., Robinson, D.G., and Denecke, J. (2001). Secretory bulk flow of soluble proteins is efficient and COPII dependent. Plant Cell **13,** 2005–2020.

Pimpl, P., Movafeghi, A., Coughlan, S., Denecke, J., Hillmer, S., and Robinson, D.G. (2000). In situ localization and in vitro induction of plant COPI-coated vesicles. Plant Cell **12,** 2219–2235.

Presley, J.F., Cole, N.B., Schroer, T.A., Hirschberg, K., Zaal, K.J.M., and Lippincott-Schwartz, J. (1997). ER-to-Golgi transport visualised in living cells. Nature **389,** 81–85.

Ritzenthaler, C., Nebenführ, A., Movafeghi, A., Stussi-Garaud, C., Behnia, L., Pimpl, P., Staehelin, L.A., and Robinson, D.G. (2002). Reevaluation of the effects of brefeldin A on plant cells using tobacco Bright Yellow 2 cells expressing Golgi-targeted green fluorescent protein and COPI antisera. Plant Cell **14,** 237–261.

Robineau, S., Chabre, M., and Antonny, B. (2000). Binding site of brefeldin A at the interface between the small G protein ADP-ribosylation factor 1 (ARF1) and the nucleotide-exchange factor *Sec 7* domain. Proc. Natl. Acad. Sci. USA **97,** 9913–9918.

Rossanese, O.W., Soderholm, J., Bevis, B.J., Sears, I.B., O'Connor, J., Williamson, E.K., and Glick, B. (1999). Golgi structure with transitional endoplasmic reticulum organisation in *Pichia pastoris* and *Saccharomyces cerevisiae*. J. Cell Biol. **145,** 69–81.

Rothman, J.E., and Wieland, F.T. (1996). Protein sorting by transport vesicles. Science **272,** 227–234.

Saint-Jore, C.M., Evins, J., Brandizzi, F., Batoko, H., Moore, I., and Hawes, C. (2002). Redistribution of membrane proteins between the Golgi apparatus and the endoplasmic reticulum in plants is reversible and not dependent on cytoskeleton networks. Plant J. **29,** 661–679.

Sambrook, J., Fritsch, E.F., and Maniatis, T. (1989). Molecular Cloning: A Laboratory Manual. (Cold Spring Harbor, NY: Cold Spring Harbor Laboratory Press).

Satiat-Jeunemaitre, B., Cole, L., Bourett, T., Howard, R., and Hawes, C. (1996a). Brefeldin A effects in plant and fungal cells: Something new about vesicle trafficking? J. Microsc. **181,** 162–177.

Satiat-Jeunemaitre, B., Steele, C., and Hawes, C. (1996b). Golgi-membrane dynamics are cytoskeleton dependent: A study on Golgi stack movement induced by brefeldin A. Protoplasma **191,** 21–33.

Schekman, R., and Orci, L. (1996). Coat proteins and vesicle budding. Science **271,** 1526–1533.

Schindler, T., Bergfeld, R., Hohl, M., and Schopfer, P. (1994). Inhibition of Golgi-apparatus function by brefeldin-A in maize coleoptiles and its consequences on auxin-mediated growth, cell-wall extensibility and secretion of cell-wall proteins. Planta **192,** 404–413.

Seemann, J., Jokitalo, E., Pypaert, M., and Warren, G. (2000). Matrix proteins can generate the higher order architecture of the Golgi apparatus. Nature **407,** 1022–1026.

Staehelin, L.A., and Driouich, A. (1997). Brefeldin A effects in plants: Are different Golgi responses caused by different sites of action? Plant Physiol. **114,** 401–403.

Storrie, B., and Yang, W. (1998). Dynamics of the inter-phase mammalian Golgi complex as revealed through drugs producing reversible Golgi disassembly. Biochim. Biophys. Acta **1404,** 127–137.

Takeuchi, M., Ueda, T., Sato, K., Abe, H., Nagata, T., and Nakano, A. (2000). A dominant negative mutant of Sar1 GTPase inhibits protein transport from the endoplasmic reticulum to the Golgi apparatus in tobacco and *Arabidopsis* cultured cells. Plant J. **23,** 517–525.

Törmäkangas, K., Hadlington, J.L., Pimpl, P., Hillmer, S., Brandizzi, F., Teeri, T.H., and Denecke, J. (2001). A vacuolar sorting domain may also influence the way in which proteins leave the endoplasmic reticulum. Plant Cell **13,** 2021–2032.

Toyooka, K., Okamoto, T., and Minamikawa, T. (2000). Mass transport of preform of a KDEL-tailed cysteine proteinase (SH-EP) to protein storage vacuoles by endoplasmic reticulum-derived

vesicle is involved in protein mobilization in germinating seeds. J. Cell Biol. **148,** 453–463.

Ueda, K., Matsuyama, T., and Hashimoto, T. (1999). Visualisation of microtubules in living cells of transgenic *Arabidopsis thaliana*. Protoplasma **206,** 201–206.

Ward, T.H., Polishchuk, R.S., Caplan, S., Hirschberg, K., and Lippincott-Schwartz, J. (2001). Maintenance of Golgi structure and function depends on the integrity of ER export. J. Cell Biol. **155,** 557–570.

Wee, E.G.T., Sherrier, D.J., Prime, T.A., and Dupree, P. (1998). Targeting of active sialyltransferase to the plant Golgi apparatus. Plant Cell **10,** 1759–1768.

Whiteheart, S.W., Rossnagel, K., Buhrow, S.A., Brunner, M., Jaenicke, R., and Rothman, J.E. (1994). *N*-Ethylmaleimide-sensitive fusion protein: A trimeric ATPase whose hydrolysis of ATP is required for membrane fusion. J. Cell Biol. **126,** 945–954.

Wood, S.A., Park, J.E., and Brown, W.J. (1991). Brefeldin-A causes a microtubule-mediated fusion of the *trans*-Golgi network and early endosomes. Cell **67,** 591–600.

Zaal, K.J.M., Smith, C.L., Polishchuk, R.S., Altan, N., Cole, N.B., Ellenberg, J., Hirschberg, K., Presley, J.F., Roberts, T.H., Siggia, E., Phair, R.D., and Lippincott-Schwartz, J. (1999). Golgi membranes are absorbed into and reemerge from the ER during mitosis. Cell **99,** 589–601.